

## Dynamic resilience assessment and emergency strategy optimization of natural gas compartments in utility tunnels

Bai, Yiping; Wu, Jiansong; Yuan, Shuaiqi; Reniers, Genserik; Yang, Ming; Cai, Jitao

**DOI**

[10.1016/j.psep.2022.07.008](https://doi.org/10.1016/j.psep.2022.07.008)

**Publication date**

2022

**Document Version**

Final published version

**Published in**

Process Safety and Environmental Protection

**Citation (APA)**

Bai, Y., Wu, J., Yuan, S., Reniers, G., Yang, M., & Cai, J. (2022). Dynamic resilience assessment and emergency strategy optimization of natural gas compartments in utility tunnels. *Process Safety and Environmental Protection*, 165, 114-125. <https://doi.org/10.1016/j.psep.2022.07.008>

**Important note**

To cite this publication, please use the final published version (if applicable).  
Please check the document version above.

**Copyright**

Other than for strictly personal use, it is not permitted to download, forward or distribute the text or part of it, without the consent of the author(s) and/or copyright holder(s), unless the work is under an open content license such as Creative Commons.

**Takedown policy**

Please contact us and provide details if you believe this document breaches copyrights.  
We will remove access to the work immediately and investigate your claim.

***Green Open Access added to TU Delft Institutional Repository***

***'You share, we take care!' - Taverne project***

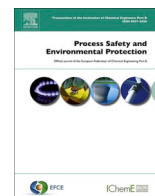
**<https://www.openaccess.nl/en/you-share-we-take-care>**

Otherwise as indicated in the copyright section: the publisher is the copyright holder of this work and the author uses the Dutch legislation to make this work public.



Contents lists available at ScienceDirect

# Process Safety and Environmental Protection

journal homepage: [www.journals.elsevier.com/process-safety-and-environmental-protection](http://www.journals.elsevier.com/process-safety-and-environmental-protection)

## Dynamic resilience assessment and emergency strategy optimization of natural gas compartments in utility tunnels

Yiping Bai<sup>a,b</sup>, Jiansong Wu<sup>a,\*</sup>, Shuaiqi Yuan<sup>b</sup>, Genserik Reniers<sup>b,c,d,\*\*</sup>, Ming Yang<sup>b</sup>, Jitao Cai<sup>a</sup><sup>a</sup> School of Emergency Management and Safety Engineering, China University of Mining & Technology-Beijing, Beijing, China<sup>b</sup> Safety and Security Science Group, Delft University of Technology, Delft, the Netherlands<sup>c</sup> Faculty of Applied Economics, Antwerp Research Group on Safety and Security (ARGoSS), Universiteit Antwerpen, Antwerp, Belgium<sup>d</sup> CEDON, KULeuven, Brussels, Belgium

### ARTICLE INFO

#### Keywords:

Resilience assessment  
Utility tunnel  
Natural gas  
Safety barrier  
Emergency strategy optimization

### ABSTRACT

As a kind of critical infrastructure of energy transportation, so-called ‘utility tunnels’ have been developed around the world. Hosting a natural gas pipeline inside the natural gas compartment of a utility tunnel facilitates its maintenance but also brings potential explosion concerns due to the confined space. Although some work focuses on the risk analysis of the natural gas pipeline inside utility tunnels, a resilience assessment is needed for dynamically modeling leakage with interacting safety barriers. In this paper, a resilience assessment model of the natural gas compartment of utility tunnels is elaborated based on numerical simulation considering interacting barrier modeling, including sensors, a ventilation system, and the possibility of emergency shutdown. Based on the calculated (natural gas compartment) resilience for casualty and economic loss, ventilation strategies and sensor layouts can be recommended and optimization is possible. Meanwhile, the delay effect of safety barriers is investigated in this work, and the unequal interval layouts of sensors are explored and proven to be effective without any further cost. The proposed resilience assessment model can be important to further improve the safety management of utility tunnels and other confined spaces where hazardous gases are transported.

### 1. Introduction

The utility tunnel (also called underground utility tunnel, multi-purpose utility tunnel, and urban utility tunnel) is a kind of underground structure hosting multiple pipelines (natural gas, water, sewer, telecommunication, electricity, heat, drainage, etc.) to prevent excavation during maintenance and facilitate daily detection (Fig. 1). As an efficient arrangement of lifelines in cities, chemical parks, and airports, the utility tunnel was used for more than one century worldwide (Bai et al., 2020; Cano-Hurtado and Canto-Perello, 1999; Wang et al., 2018). Since the increasing attention of sustainable development of urban underground space, the utility tunnel reached a boom period in the latest decade. However, laying a natural gas pipeline in a confined space also brings a higher possibility of gas accumulation which can result in a fire or an explosion in the case of insufficient ventilation. Such gas accidents can not only stop the supply of natural gas but also affect adjacent pipelines inside utility tunnels and threaten activities on the ground or even result in a breakdown of the whole lifeline system (Wu et al., 2021).

In 2021, around 600 m<sup>3</sup> of natural gas leaked and accumulated in a relatively confined riverway under a market, resulting in a catastrophic explosion with 26 deaths and 138 injuries in Shiyuan, China (Department of Emergency Management of Hubei Province, 2021). In 2015, around 5000 people were evacuated due to gas leakage and fire in an underground utility tunnel in London (Highways, 2015). In 2014, the propylene leakage and accumulation in drainage culverts resulted in a series of explosions with 32 fatalities and 321 injuries in Kaohsiung, China (Liaw, 2016). Therefore, the safety and resilience of natural gas pipelines inside utility tunnels deserve attention from the academic world.

Many risk assessment approaches focus on natural gas pipelines, but only a few on the natural gas pipeline inside underground utility tunnels (Vairo et al., 2021; Wu et al., 2017). Although the medium transferred through pipelines is the same, there are still many differences between natural gas pipelines inside utility tunnels and those buried directly. Fig. 2 illustrates a schematic diagram of the natural gas compartment of utility tunnels based on a national standard (GB50838, 2015). The

\* Corresponding author.

\*\* Corresponding author at: Safety and Security Science Group, Delft University of Technology, Delft, the Netherlands.

E-mail addresses: [jiansongwu@cumbt.edu.cn](mailto:jiansongwu@cumbt.edu.cn) (J. Wu), [G.L.L.M.E.Reniers@tudelft.nl](mailto:G.L.L.M.E.Reniers@tudelft.nl) (G. Reniers).

<https://doi.org/10.1016/j.psep.2022.07.008>

Received 12 April 2022; Received in revised form 1 July 2022; Accepted 4 July 2022

Available online 8 July 2022

0957-5820/© 2022 Published by Elsevier Ltd on behalf of Institution of Chemical Engineers.

natural gas pipeline is required to be arranged in a separate compartment (i.e., a natural gas compartment) of utility tunnels with a ventilation system, and the natural gas compartment is separated by firewalls and fire doors every 200 m with flammable gas sensors, a mechanical ventilation system, sprinklers, extinguishers, and a control cabinet inside. A positive aspect of this approach is that corrosion or third-party damage that significantly affects buried gas pipelines do not attribute much to gas pipelines inside utility tunnels. A negative aspect however of this way of work is that the natural gas compartment of utility tunnels is a confined space where gas leakage can directly accumulate and may result in a fire or explosion in the case of insufficient ventilation. Therefore, sensor detection, ventilation, emergency shutdown, fire zone, evacuation, etc., are essential and influential factors for the safety of utility tunnels.

However, the relevant accidents, operation data, or management experience are too scarce to support the risk assessment and safety management of utility tunnels since the boom of large-scale multi-compartment underground utility tunnels just emerged in the last decade. Recently, for the safety analysis of gas pipelines inside utility tunnels, there have been hazard identification techniques (Bai et al., 2020), index-based approaches (Canto-Perello et al., 2013), probabilistic models (Fang et al., 2019; Wu et al., 2021), experiments (Ye et al., 2021; Zhao et al., 2022) and numerical simulations (Cai et al., 2022; Wu et al., 2020) conducted. The index-based approaches like the analytic hierarchy process (AHP) are easy to integrate with other tools and practical for application in reality. Still, they can only realize static and semi-quantitative analysis. Probabilistic methods like Bayesian network, event tree, and bow-tie can quantify the probability of events but rely much on expert judgments (Amin et al., 2019). Although the experiment analysis is more objective and involves few personal opinions, it is extremely time-consuming, expensive, and can only deal with simplified scenarios. Also, for a utility tunnel, a large-scale infrastructure, it is not possible to experiment on a real scale, and the results of small-scale tests cannot be directly applied in practice (Zhao et al., 2022). Although some numerical simulation research was conducted to analyse natural gas leakage, diffusion, and explosion inside utility tunnels to optimize pipeline allocation, fire zone, or safety barriers (Baalisampang et al., 2019; Bu et al., 2021; Xu et al., 2021). But these studies focus more on the gas dispersion behavior, gas concentration field, explosion overpressure, and corresponding physical mechanism instead of comprehensive system performance. And the current work has not reached the resilience analysis of the whole natural gas compartment system considering sensor detection, ventilation, and shutdown simultaneously.

Recently, resilience has been attracting significant attention and has been considered to be a critical property for system operation with a temporal evolution (Bento et al., 2021; Duchek, 2020). Generally, by considering the ability of disruption, absorption (degradation), adaption (learning), restoration, and their impact on the performance of a system,

a resilience curve can be determined (Ahmadi et al., 2021; Chen et al., 2021; Pawar et al., 2021). Resilience analysis was conducted in many fields, including the energy and process industry (Hu et al., 2021; Sang et al., 2021), environment (Saikia et al., 2022; Yao et al., 2022), construction (Peñalosa et al., 2021), economy (Zhu et al., 2021), transportation (Serdar et al., 2022), medicine (Brittain et al., 2021), etc. Due to the capability of dynamic updating and quantitative predicting, the dynamic Bayesian network (DBN) has been widely used for resilience modeling (B. Cai et al., 2021; Sarwar et al., 2018; Zhang et al., 2021). Also, many approaches apply the data envelopment analysis (DEA) (Azadeh and Salehi, 2014; Azadeh et al., 2014, 2017; Salehi and Veitch, 2020).

Up to now, there are few resilience studies on the utility tunnel, since it is a complex system with various pipelines and safety barriers inside. There are already a few studies on the resilience assessment of directly buried natural gas pipelines (Emenike and Falcone, 2020), but cannot be applied to the natural gas compartment of the utility tunnel which is a confined space with multiple interacted safety barriers. Marino and Zio (2021) have proposed a resilience analysis framework of natural gas pipelines from a cyber-physical perspective considering traditional physical failure (spilling, jet fire, and VCE) and cyber-attack. Sesini et al. (2020) applied linear programming to analyse natural gas supply resilience on a large scale. Su et al. (2018) integrated Markov chains and graph theory to assess the reliability of natural gas networks stochastically. Psyras and Sextos (2018) reviewed the previous resilience assessments of buried gas pipelines and emphasized the impact of ground deformations. Also, some researchers analysed various potential faults and modeled the running of gas networks with empirical or simplified equations (Golar and Esmaily, 2017; Dell'Isola et al., 2020)). Meanwhile, most of the current resilience studies of natural gas networks focused on long-distance transmission systems instead of the urban distribution network (Liu and Song, 2020).

It seems that there is still a lack of a dynamic resilience assessment approach of the natural gas compartment in utility tunnels considering sensor detection, ventilation, and emergency shutdown (ESD) simultaneously. By integrating computational fluid dynamics (CFD) and resilience theory, a resilience assessment model for the natural gas compartment of utility tunnels is proposed. The proposed approach can efficiently model the gas leakage with interacting safety barrier behaviors to quantitatively assess the system resilience. The results of this work can not only put forward specific optimization of safety barriers to support the safety management of utility tunnels but also can be applied to other tunnel spaces where hazardous gas may leak.

## 2. Methodology

In this section, the proposed dynamic resilience assessment approach is introduced in detail, including a general framework, interacting

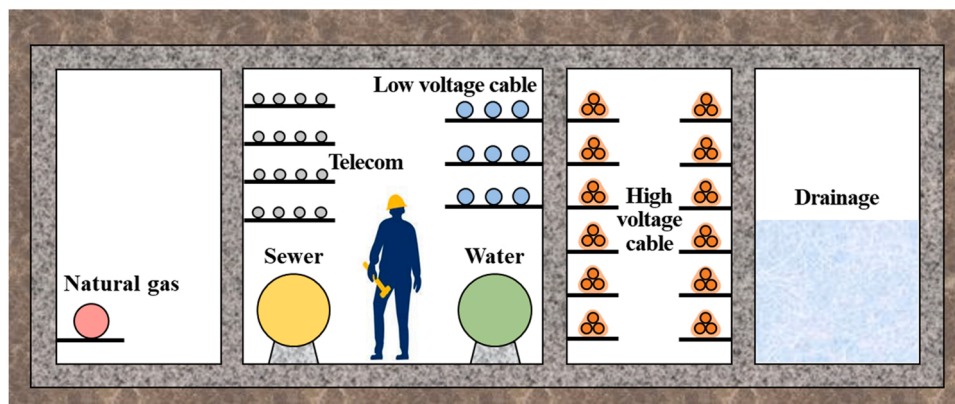


Fig. 1. Schematic diagram of the cross-section of a utility tunnel.

barrier modeling, simulation of gas leakage and dispersion, safety performance assessment, and resilience-based optimization.

2.1. Methodology framework

As shown in Fig. 3, there are generally four parts of the proposed resilience assessment model. First, interacting behaviors of multiple safety barriers (sensors, ventilation system, ESD) inside utility tunnels are analysed and modeled to determine their potential influence on gas leakage and dispersion. Second, a computational fluid dynamics (CFD) method is introduced to simulate the gas leakage and dispersion considering multi-barrier influence to obtain the spatial and temporal distribution of gas concentration in the natural gas compartment. Third, the consequence indexes of gas concentration are determined to calculate the dynamic safety performance index based on the spatial and temporal distribution of gas concentration. Finally, based on the dynamic safety performance, the temporal resilience index of the natural gas compartment of a utility tunnel can be obtained. Then, resilience-based optimization analysis is conducted through case studies. The details of each part are elaborated in the following sections.

2.2. Interacting barrier modeling

The primary safety barriers inside the natural gas compartment of utility tunnels are sensors of hazardous gas, ventilation systems (mechanical ventilation fans at each end of the compartment), emergency shutdown systems (ESD) (including auto-ESD and manual-ESD), fire doors, firewalls, and extinguishers. Based on a national regulation (GB50838, 2015), the behaviors of safety barriers inside the natural gas compartment of utility tunnels in the different gas concentrations are illustrated in Fig. 4. During the normal operation of the natural gas compartment of utility tunnels, the air exchange volume in one hour should be 6 times the volume of the whole compartment (GB50838, 2015). It means the average air velocity of ordinary ventilation should be 0.333 m/s ( $200 \times 3 \times 1.8 \times 6 / (3 \times 1.8 \times 3600)$ ) at the cross-section. In the case of an emergency (i.e., gas concentration higher than 1% VOL), the air exchange volume will double to 12 times per hour, which means the air velocity of emergency ventilation should be 0.667 m/s at the cross-section. And the ESD will be activated when the concentration reaches 25% VOL of the lower explosive limit (i.e., 1.25% VOL for natural gas). Also, the gas cloud will explode when the gas concentration is between 5% VOL and 15% VOL (Wang et al., 2020), and the ignition source appears simultaneously in the same area.

Since there usually are 14 flammable gas sensors in one fire zone (of 200 m) of the natural gas compartment, there are  $2^{14}$  (i.e., 16,384) potential combinations of sensor states, and therefore it is impossible to use an event tree approach or other scenario-based methods. Also, because the behaviors of the ventilation system and ESD are all related to the alarm of sensors, and the interactions among them are complicated, the interacting barrier modeling approach is proposed in this work. The logic flow chart of the barrier interactions is shown in Fig. 5.

As Fig. 5 shows, the modeling of this study starts with gas leakage and ends with a gas explosion with multiple safety barriers and their corresponding actions during the period. The output of this barrier

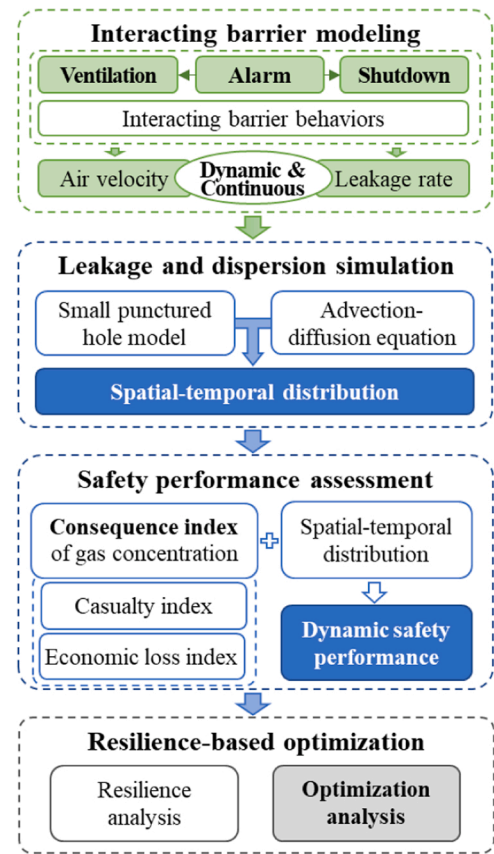


Fig. 3. Methodology framework of the resilience assessment model.

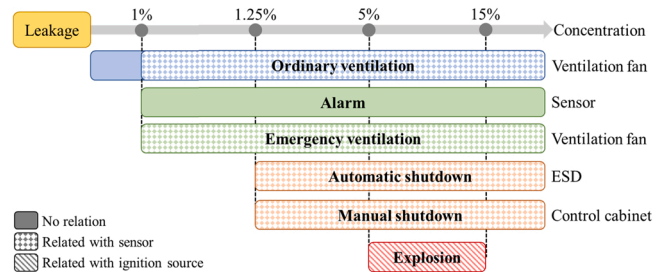


Fig. 4. Behaviors of safety barriers inside natural gas compartment.

modeling is the change of air velocity and leakage rate. Based on the national regulation (GB50838, 2015) and previous work (Cai et al., 2022), the air velocity of inlet (Eq.1) is set as 0.333 m/s and 0.667 m/s for normal ventilation and emergency ventilation, respectively. Based on the previous work (Liu et al., 2019; Yang et al., 2020; Yuan et al., 2019;), the dynamic leakage rate change is determined as Eq.2 to Eq.4 and then inputted into the following gas dispersion simulation work.

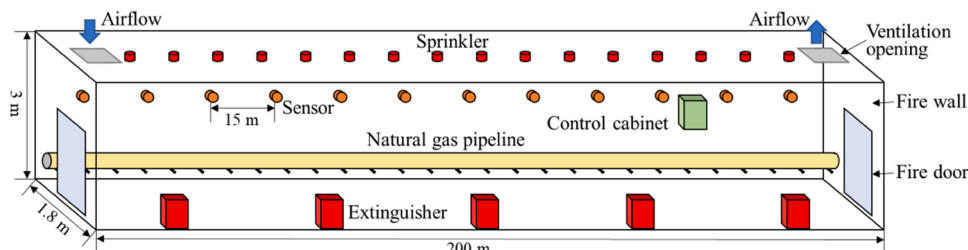


Fig. 2. Schematic diagram of a natural gas compartment of utility tunnels.

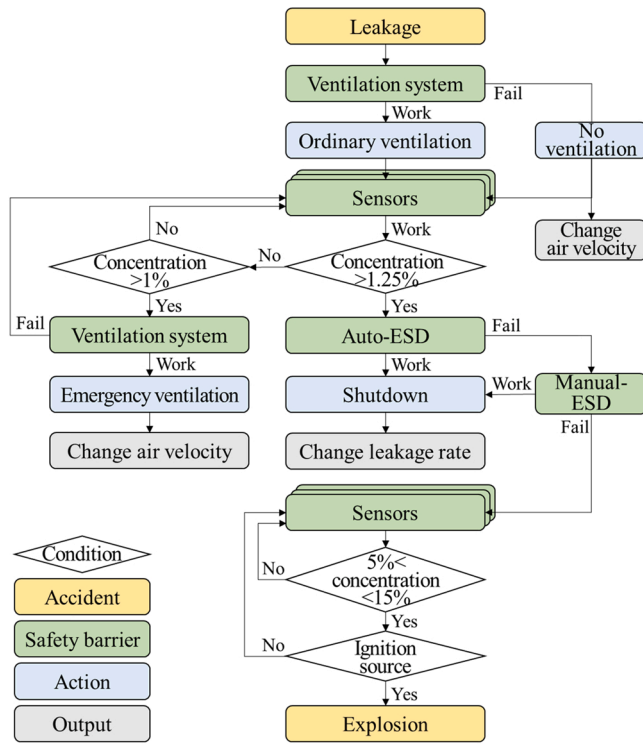


Fig. 5. Logic flow chart of barrier interactions.

term of leakage,  $dx$  is the distance step of Eq.5 (1 m in this work), and the time step of Eq.5 is set as 1 s for simulation.

$$\frac{\partial c}{\partial t} + \frac{\partial(uc)}{\partial x} = \frac{\partial}{\partial x} \left( D \frac{\partial c}{\partial x} \right) + q \quad (5)$$

$$q = \frac{Q_E}{\rho A_L dx} \quad (6)$$

As the simulation of gas leakage and dispersion inside the natural gas compartment of utility tunnels is validated as an efficient tool, the obtained spatial and temporal distribution of gas concentration will be inputted into the following safety performance assessment part (J.T. Cai et al., 2021; Yuan et al., 2019).

### 2.4. Safety performance assessment

Based on the previous sections, the spatial and temporal distribution of gas concentration in the natural gas compartment is obtained. However, only gas concentration obtained by numerical simulation cannot comprehensively reflect the safety performance of natural gas compartments. So the potential ‘casualty curve’ and ‘economic loss curve’ of different gas concentrations are proposed in this paper to calculate the temporal safety performance index.

For the casualty curve, the explosion overpressure and the asphyxia effect are considered. A gas cloud of a particular volume is assumed in the natural gas compartment to assess the potential consequences of different gas concentrations to determine the casualty index function. Based on the experimental results (Pekalski et al., 2005), the explosion overpressure curve of methane-air mixtures can be determined. According to the previous work about the gas explosion in the utility tunnel, a hundred-cubic gas cloud can result in an overpressure around 21 kPa for 6.5% VOL and 14% VOL volume concentration, 33kPa for 8% VOL concentration, 68 kPa for 10% VOL concentration (Yan et al., 2020; Yang et al., 2021; Zhang et al., 2020; Zhu et al., 2020). Based on the data from Health and Safety Executive (2010), exposure to higher than 21 kPa is fatal for humans inside, and 70 kPa overpressure leads to 100% fatality (Table 1). Therefore, the overpressure function and fatality ratio can be measured to obtain the casualty curve of different gas concentrations (blue line in Fig. 6). Though methane is nontoxic, a high concentration of methane can displace oxygen in the air and may result in asphyxia. According to the consequence of exposure to different oxygen concentrations for humans (Sciencing, 2018), potential asphyxia effects of different gas concentrations can be determined, as Table 2 shows. Therefore, the 100% fatality corresponds to 71.5% VOL gas concentration (6% VOL oxygen concentration), 50% fatality corresponds to 52.4% VOL concentration, and 10% fatality to 33.3% VOL concentration. So the casualty curve of asphyxia is determined as the black line in Fig. 6.

For the potential economic loss of gas accidents in the utility tunnels, blast damage to equipment and gas outage loss after the emergency shutdown are taken into account. Based on the data of blast damage for building structures (FEMA, 2003), the damage approximations of overpressure to tunnel structures are determined in Table 3. And the damage probability of pipelines inside utility tunnels is determined in Table 4 according to the work of Cozzani and Salzano (2004). Based on the investment estimation of utility tunnel construction shown in Table 5 and relevant gas pipeline construction cost shown in Table 6 (MOHURD, 2015), the consequences of gas explosion can be obtained as the blue line of Fig. 7. Due to the diversity and uncertainty of end-users,

Table 1  
Explosion overpressure effects.

Overpressure (kPa)	Fatality ratio
21	20%
35	50%
70	100%

$$V_{inlet} = \frac{n \times V_{total}}{60 \times 60 \times A_{cs}} \quad (1)$$

$$Q_0 = CA_L P_0 \sqrt{\frac{Mk}{RT} \left( \frac{2}{k+1} \right)^{\frac{k+1}{k}}} \quad (2)$$

$$Q_E = Q_0 \exp \left( \frac{-Q_0}{m_0 d} (t - t_E) \right) \quad (3)$$

$$m_0 = A_L L \rho \quad (4)$$

Where  $n$  is the times of air exchange per hour (6 for ordinary and 12 for emergency),  $V_{total}$  is the total volume of the gas compartment,  $S_{cs}$  is area of cross-section of the gas compartment,  $Q_0$  is the initial leakage rate,  $C$  is the leakage coefficient,  $A_L$  is the area of leakage hole,  $P_0$  is the initial pressure of the gas pipeline,  $M$  is the molecular weight of the natural gas,  $k$  is the ratio of specific heats,  $R$  is the universal gas constant,  $T$  is temperate of the natural gas,  $Q_E$  is the leakage rate after ESD activation,  $m_0$  is the mass of gas,  $t_E$  is the time of ESD activation,  $L$  is the distance between ESD valve and leakage position,  $\rho$  is the density of natural gas.

### 2.3. Simulation of gas leakage and dispersion

With the interacting barrier behaviors and corresponding changes of simulation input parameters determined in the previous section, gas leakage and dispersion simulation were conducted in this study. Because the small hole leakage scenario is the dominant pattern of pipeline leakage, small punctured hole modeling is applied in this work (Dong et al., 2003). Since the natural gas compartment inside a utility tunnel is a long and narrow space (3 \*1.8 \*200 meter in this work), gas leakage and dispersion inside the natural gas compartment can be simplified as a one-dimensional scenario with 200 spatial steps. Therefore, the governing equation in this work is the one-dimensional advection-diffusion equation (Eq.5 and Eq.6) based on Yuan et al. (2019).  $c$  is the average gas concentration of the cross-section of the natural gas compartment,  $u$  is the mean airflow velocity,  $D$  is the diffusion coefficient,  $q$  is the source

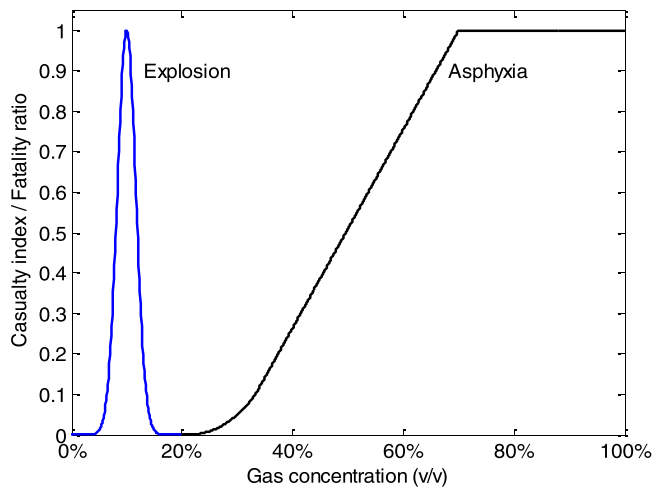


Fig. 6. Casualty index of gas concentration.

**Table 2**  
Asphyxia effects of different gas concentration.

Oxygen concentration	Consequences	Gas concentration
14% VOL	Mental functions impaired, and respiration intermittent	33.3% VOL
10% VOL	Collapse and unconscious	52.4% VOL
6% VOL	Die	71.5% VOL

**Table 3**  
Damage approximations of explosion overpressure to the tunnel structure.

Damage	Overpressure/kPa
Cable shelf failure	7.6–12.4
Severe damage to steel framed buildings	27.6–48.3
Severe damage to reinforced concrete structures	41.4–62.1
Probable total destruction of most buildings	68.9–82.7

**Table 4**  
Probability of overpressure damage to pipelines.

Overpressure/kPa	Damage	Damage probability
7	Failure of connection	1%
20	Displacement of steel supports	10%
37.4	Catastrophic failure of pipe supports	30%
42	Pipeline failure	30%
47	Failure of non-pressure equipment	99%

**Table 5**  
Cost estimation of utility tunnel structure construction.

Cross-section area / m <sup>2</sup>	Compartments	Construction cost / (yuan/m)
10–20	1	51,091–61,133
20–35	1	61,133–75,557
20–35	2	61,133–97,815
35–45	2	97,815–122,121
35–45	3	97,815–139,953
35–45	4	97,815–163,742

the gas outage loss cannot be determined in a universal way. Therefore, the outage loss is assumed as 1 million yuan (143,000 euros) in this work, and it can be further adjusted in a particular case. Since the shutdown threshold of the gas pipeline in the utility tunnel is 1.25% VOL of methane detection, the outage loss curve is a horizontal line as the black line of Fig. 7. After normalization and summing up, the economic

**Table 6**  
Cost estimation of gas pipeline inside utility tunnels.

Pipe diameter / mm	Installation cost / (yuan/m)	Equipment cost / (yuan/m)	Other cost / (yuan/m)	Total cost / (yuan/m)
200	982	285	336	1603
300	1318	285	424	2027
400	1584	285	495	2364
500	1922	285	585	2792

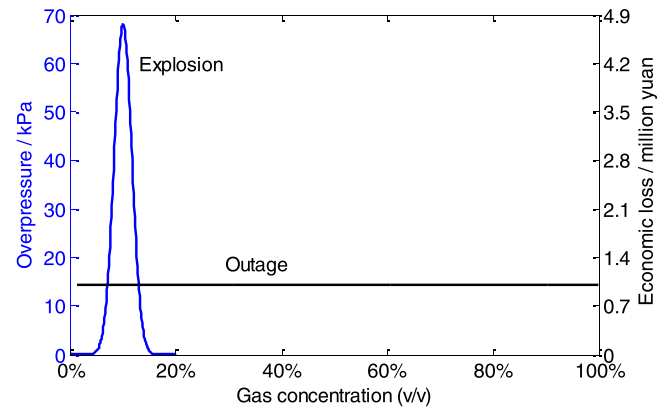


Fig. 7. The consequence of gas explosion and outage in different gas concentrations (the left y-axis is equivalent to the right one).

loss curve of gas concentration is determined in Fig. 8.

Based on the casualty curve and economic loss curve in Fig. 6 and Fig. 8, the casualty index and economic loss index of each position (discretized every meter) can be calculated. By summing up corresponding indexes of all positions, the cumulative consequence index of the whole compartment can be obtain. Finally, the safety performance index can be quantified by subtracting the cumulative consequence index from the initial performance value, which is determined based on the cumulative consequence index in the worst case. Therefore, the dynamic safety performance index can be generally shown in Fig. 9. The resilience index can be calculated as Eq.7 shows.

$$R = \frac{\int_{t_0}^{t_3} P(t) dt}{P(t_0) \times (t_3 - t_0)} \quad (7)$$

Where  $P(t)$  is the safety performance index at moment  $t$ ;  $t_0$  is the time

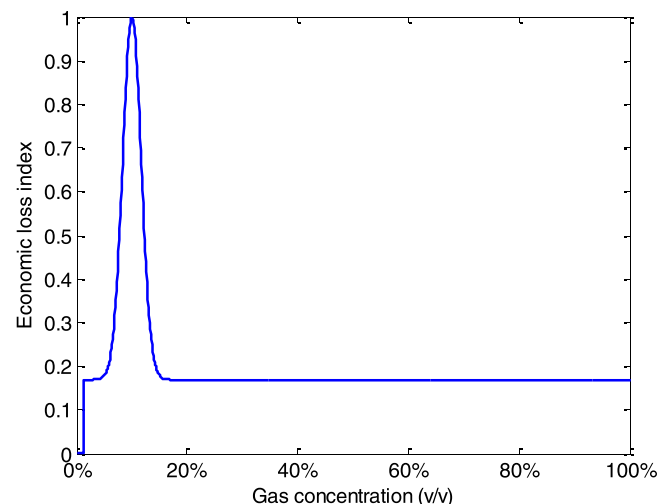


Fig. 8. Economic loss index of gas concentration.

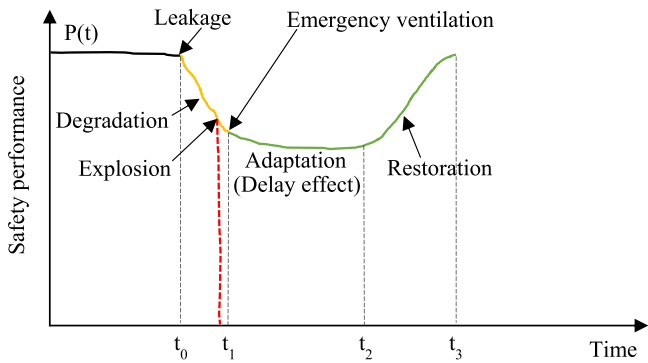


Fig. 9. A schematic safety performance curve of the natural gas compartment.

when the disruption starts (i.e., leakage in this work);  $t_1$  is the time when the emergency response is activated;  $t_2$  is the time when the performance starts to recover (i.e., due to the delay effect of safety barriers in this work);  $t_3$  is the time when the performance reaches the acceptable performance.

### 3. Case study

Based on the proposed resilience assessment approach of the natural gas compartment in utility tunnels, case studies are conducted as follows to dynamically assess the resilience and optimize safety barriers inside utility tunnels.

#### 3.1. Configuration

Because methane is the main component of natural gas transferred through utility tunnels, the media inside the gas pipeline is assumed pure methane in the case study. Since the natural gas compartment inside the utility tunnel is separated by normally-closed fire doors every 200 m, the length of the natural gas compartment is set as 200 m. Other parameters of the compartment and the pipeline are shown in Table 7.

#### 3.2. Influence of leakage location

In this section, the influence of different leakage locations is analysed with 9 cases, whose distance from the upwind end of the natural gas compartment is different, as shown in Table 8. For controlling variables, the air velocity of ordinary and emergency ventilation is set as 0.333 m/s and 0.667 m/s, which is the lower limit of Chinese national regulation (GB50838, 2015). In this section, the nearest sensor is 10 m away from the leakage source, and the simulation results indicate that it takes 20 s after the leakage to trigger emergency ventilation and ESD. As shown in Fig. 10, the closer the leakage source to the upwind end, the less resilient the natural gas compartment will be; since the natural gas will be dispersed to the downwind area by ventilation until discharged outside through a ventilation opening at the downwind end. Therefore, the leakage close to upwind will be more dangerous with a larger hazardous

Table 7

Configuration of the natural gas compartment in the utility tunnel.

Parameter	Setup value
Height of the natural gas compartment	3 m
Width of the natural gas compartment	1.8 m
Length of the natural gas compartment	200 m
Natural gas pipeline diameter	300 mm
Natural gas pipeline pressure	1.6 MPa
Natural gas temperature	293 K
Natural gas density	0.7174
Leakage hole diameter	4 mm
Distance between hole and ESD valve	1000 m
Leak moment	0 s

Table 8

Cases of different leakage locations and their resilience indexes.

Case	Leakage location	Resilience for casualty	Resilience for economic loss
1	20 m	0.8882	0.8305
2	40 m	0.9028	0.8513
3	60 m	0.9178	0.8723
4	80 m	0.9330	0.8933
5	100 m	0.9478	0.9140
6	120 m	0.9618	0.9339
7	140 m	0.9742	0.9527
8	160 m	0.9845	0.9698
9	180 m	0.9929	0.9855

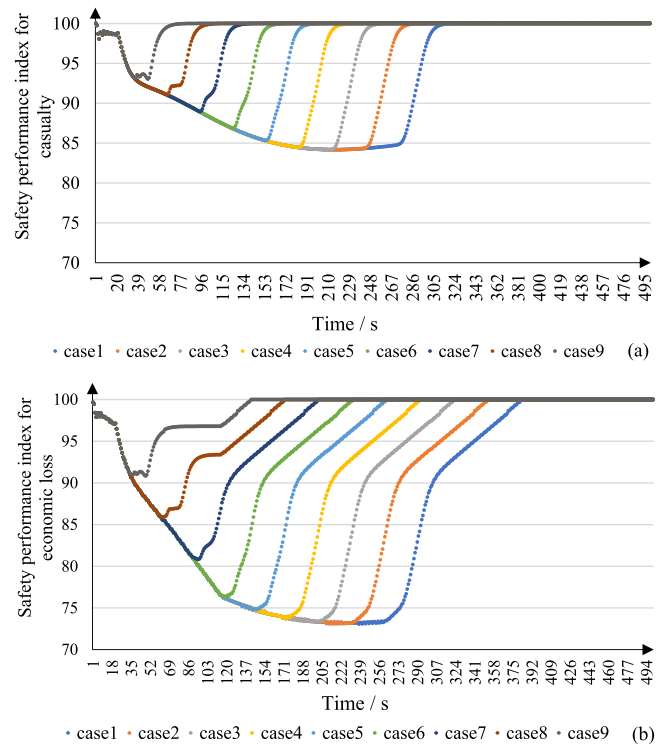


Fig. 10. Safety performance curves of different leakage locations.

gas cloud and will result in a lower resilience of the natural gas compartment. In this work, the acceptable safety performance index is set as 99.9. So resilience indexes can be calculated based on Eq. 2, and the  $t_0$  is 0 s,  $t_1$  is 20 s, and  $t_3$  are 315 s and 383 s for casualty and economic loss respectively. For a leakage located at 20 m from the upwind end, the resilience index of the natural gas compartment will drop to 0.8882 for casualty and drop to 0.8305 for economic loss.

Meanwhile, the results of Fig. 10 also indicate the delay effect of safety barriers in the natural gas compartment. Although both ESD and emergency ventilation are activated at 20 s, both safety performance index for casualty and economic loss cannot recover immediately. As for case 1, the recovery of the safety performance index starts 255 and 240 s later than safety barrier activation for casualty and economic loss, respectively. And the delay effect is related to the distance between the leakage source and the ventilation opening. There are mainly two reasons that may result in the delay effect of safety barriers: i) The gas release rate takes time to drop to 0 after ESD activation (more than 100 s in the case of a 1000-m distance between leakage hole and ESD valve), and ii) The gas dilution takes time even if the air velocity of emergency ventilation is higher than ordinary ventilation. Therefore, the delay effect of the safety barrier in the utility tunnel is identified by the proposed model and can be mitigated in the following sections.

### 3.3. Ventilation strategy analysis

Based on the results of the previous section, the delay effect of safety barriers significantly affects the resilience of the natural gas compartment of utility tunnels. One of the main reasons for the delay is insufficient ventilation, i.e., the air velocity is not high enough to quickly dilute the leaked gas. Therefore, the ventilation strategy is analysed in this section to improve the system resilience and mitigate the delay effect. First, the air velocity of ordinary ventilation is increased in cases 1, 10, 11, 12, 13 in Table 9. As shown in Fig. 11, the increase of ordinary air velocity from 0.333 m/s to 0.667 m/s can slightly mitigate the delay effect but also lower the safety performance index in the early stage of leakage. For cases 1, 10, 11, 12, and 13, the  $t_0$  is 0,  $t_1$  is 20 s, and  $t_3$  are 315 s and 383 s for casualty and economic loss respectively. Meanwhile, both the casualty resilience and the economic loss resilience in Table 9 cannot be improved dramatically in the case of strengthening ordinary ventilation, which means the ordinary ventilation does not need to be strengthened.

The ordinary ventilation is set to 0.333 m/s to analyse the effect of increasing emergency ventilation shown as cases 1, 14, 15, 16, and 17 in Table 9. The results in Fig. 12 indicate the effectiveness of increasing emergency ventilation. For the safety performance of casualty, the delay time of performance recovery reduces from 341 s for case 14–172 s for case 17 (Fig. 12 (a)). As for the safety performance of economic loss, the delay time reduces from 318 s for case 14–170 s for case 17 (Fig. 12 (b)). For cases 1, 14, 15, 16, and 17, the  $t_0$  is 0,  $t_1$  is 20 s, and  $t_3$  are 419 s and 489 s for casualty and economic loss respectively. So, the resilience for casualty increases from 0.8626 for case 14–0.9923 for case 17, and the resilience for economic loss increases from 0.8139 for case 14–0.9409 for case 17. While further improvement of emergency ventilation can still improve the resilience of the natural gas compartment, it may be too costly. So, the results demonstrate that the ventilation strategy should be set as 0.333 m/s for ordinary ventilation and 1 m/s for emergency ventilation. In this case, the safety performance index of the natural gas compartment for casualty will only slightly drop to 98 after the gas leakage, and the resilience is higher than 0.99.

### 3.4. Sensor layout analysis

Based on the determined optimal ventilation strategy (0.333 m/s for ordinary ventilation and 1 m/s for emergency ventilation), the different sensor layouts are analysed in this section to realize the resilience-based optimization of sensor layouts.

First, cases 18–24 are designed to compare the sensor layouts with different equal intervals, as shown in Table 10. As Fig. 13 shows, the safety performance index of all seven cases drops to around 99 for casualty and 85 for economic loss. Although the natural gas compartment of the utility tunnel will be more resilient with more sensors arranged, it also costs more. There is not much difference between the resilience of different sensor layouts, no matter for casualty or economic loss aspects. The results show that the current minimum limit of sensor interval

**Table 9**  
Cases of different ventilation strategies and their resilience indexes.

Case	Leakage location	Ordinary ventilation	Emergency ventilation	Resilience for casualty	Resilience for economic loss
1	20 m	0.333 m/s	0.667 m/s	0.8882	0.8305
10	20 m	0.4 m/s	0.667 m/s	0.8833	0.8261
11	20 m	0.5 m/s	0.667 m/s	0.8782	0.8210
12	20 m	0.6 m/s	0.667 m/s	0.8788	0.8199
13	20 m	0.667 m/s	0.667 m/s	0.8873	0.8247
14	20 m	0.333 m/s	0.5 m/s	0.8626	0.8139
15	20 m	0.333 m/s	0.8 m/s	0.9465	0.8979
16	20 m	0.333 m/s	0.9 m/s	0.9688	0.9194
17	20 m	0.333 m/s	1 m/s	0.9923	0.9409

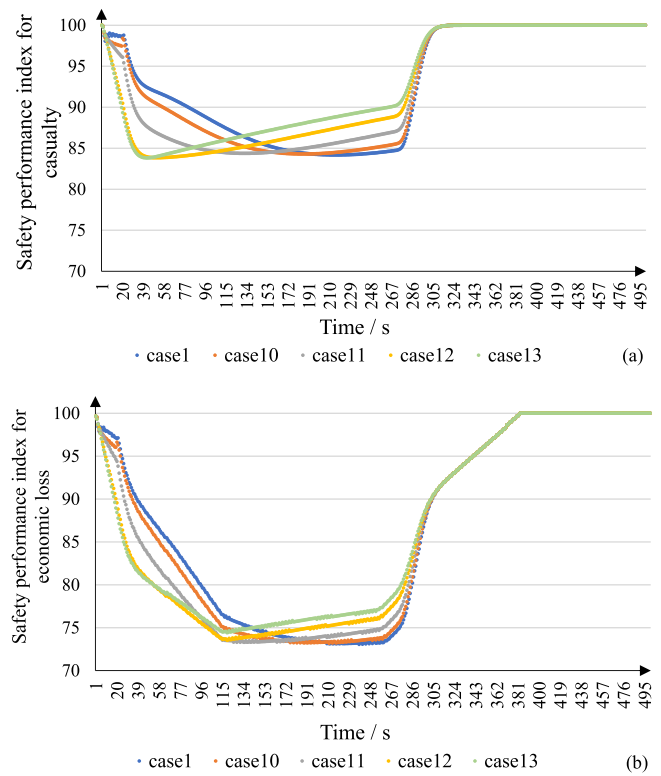


**Fig. 11.** Safety performance curves of different ordinary ventilation.

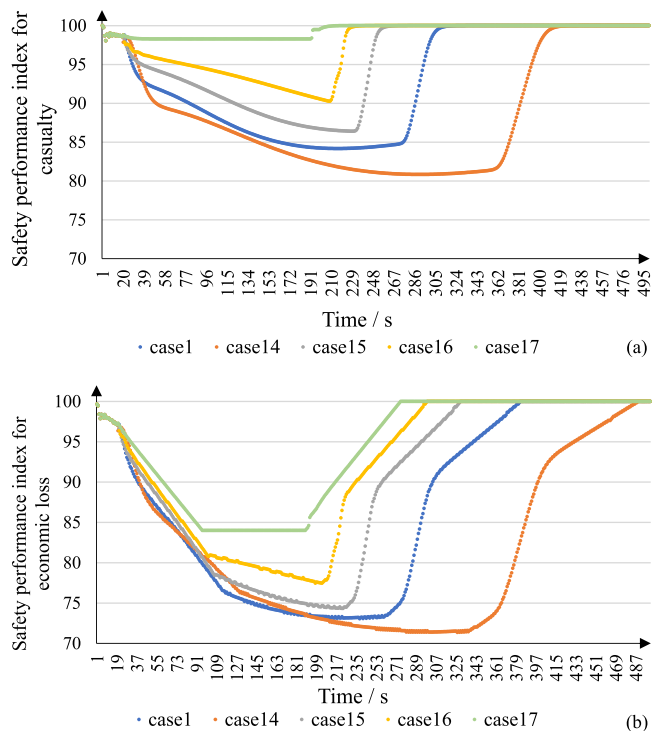


**Fig. 12.** Safety performance curves of different emergency ventilation.

(15 m) proposed by MOHURD (2011) can be changed to a lower one for utility tunnels. For cases 18–24, the  $t_0$  is 0, and  $t_3$  are 237 s and 309 s for casualty and economic loss respectively. Based on the calculated resilience indexes of the seven cases, 10 sensors equally distributed at 20-meter intervals (case 19) should be proposed as the optimal allocation among other equal-interval layouts. In this case, the resilience index

**Table 10**  
Cases of different sensor layouts and their resilience indexes.

Case	Sensor number	Layout / m	Resilience for casualty	Resilience for economic loss
18	8	equal interval (25)	0.9896	0.8967
19	10	equal interval (20)	0.9910	0.9001
20	12	equal interval (16.67)	0.9922	0.9031
21	14	equal interval (14.29)	0.9929	0.9047
22	16	equal interval (12.5)	0.9935	0.9068
23	18	equal interval (11.11)	0.9939	0.9076
24	20	equal interval (10)	0.9941	0.9078

for casualty is higher than 0.99, and that for economic loss is higher than 0.90, which means the proposed layout with 20-meter intervals does ensure the adequate resilience of the natural gas compartment. Compared with case 21 according to the current specification (15-m intervals), such change can save 28.57% sensors with only 0.19% and 0.51% resilience lost for casualty and economic loss respectively.

Although the above results show that the 20-meter interval is sufficient for a resilient natural gas compartment, the unequal intervals still need to be analysed, which do not require any further investment but only change intervals. In the following part, six unequal-interval layouts with the same number of sensors are designed as cases 25–30 in Table 11 to compare with case 19, whose intervals are equal. Since the results of the previous section indicate that the leakage on the upwind side is more dangerous than downwind ones, intervals on the upwind side are smaller than that of the downwind side. Meanwhile, each case includes 8 different leakage locations (every 25 m) to realize a comprehensive analysis of sensor layouts, since the leakage location affects the sensor alarm time and further affects the activation time of safety barriers.

(Comprehensive resilience is the average of resilience indexes of 8 leakage locations).

Fig. 14 and Fig. 15 show the safety performance curves for casualty and economic loss, respectively. On the one hand, the diversity of different curves in one sub-figure (like Fig. 14 (a)) indicates that leakage locations affect the utility tunnel resilience. On the other hand, it can be found that the safety performance curves of different cases vary by comparing different sub-figures (like Fig. 14 (a) with Fig. 14 (b)), which means the layout intervals do also affect the utility tunnel resilience. For the seven cases, the  $t_0$  is 0, and  $t_3$  are 271 s and 322 s for casualty and economic loss respectively. For comprehensively quantifying the resilience of different sensor layouts, the average of resilience indexes of 8 curves in one sub-figure is calculated as comprehensive resilience, as shown in Table 11. The results show that case 27 has the highest comprehensive resilience of both casualty and economic loss, which are 0.9963 and 0.9541, respectively. Although the comprehensive resilience varies little between different layouts with the same number of sensors, the unequal-interval layout can improve the resilience without further

cost. In this work, the proposed optimal sensor layout should be 10 sensors in a 200-m compartment arranged in an arithmetic progression interval:  $8.75 + 2.5(n-1)$ , where n is the number of sensors from 1 to 10.

**4. Discussion**

As shown in Section 3.2, the activation of safety barriers (emergency ventilation and ESD system) inside the natural gas compartment has a significant delay effect, which means system performance cannot start to recover simultaneously with the sensor alarm. Meanwhile, since the emergency ventilation facilitates the spread of leaked gas over a larger area, the system performance will drop for a period right after emergency ventilation activation. For example, in some cases, the high gas concentration (higher than the upper explosive limit) could drop to a concentration within the lower and upper explosive limit for a period after the emergency ventilation activation. Both the facts indicate that the staff should be on alert even after successfully activating the safety barriers. And the emergency ventilation should be maintained for a sufficient time to remove all the leaked gas inside the compartment.

The results in Section 3.3 and Section 3.4 indicate that the current specification of emergency ventilation is insufficient and that of the sensor is excessive. The optimal ventilation strategy and sensor layout are proposed based on the comparative analysis of several cases. Since the safety performance curve varies for different leakage locations,

**Table 11**  
Cases of different sensor layouts and their resilience indexes.

Case	Sensor number	Interval of sensors / m	Comprehensive resilience for casualty	Comprehensive resilience for economic loss
19	10	equal	0.9934	0.9473
25	10	progression: 20 arithmetic	0.9953	0.9515
26	10	progression: 16.4 + 0.8(n-1) arithmetic	0.9947	0.9505
27	10	progression: 12.35 + 1.7(n-1) arithmetic	0.9963	0.9541
28	10	progression: 8.75 + 2.5(n-1) geometric	0.9932	0.9473
29	10	progression: 15.9 * 1.05 <sup>n-1</sup> geometric	0.9938	0.9488
30	10	progression: 12.55 * 1.1 <sup>n-1</sup> geometric	0.9929	0.9464
		progression: 7.7 * 1.2 <sup>n-1</sup> geometric		

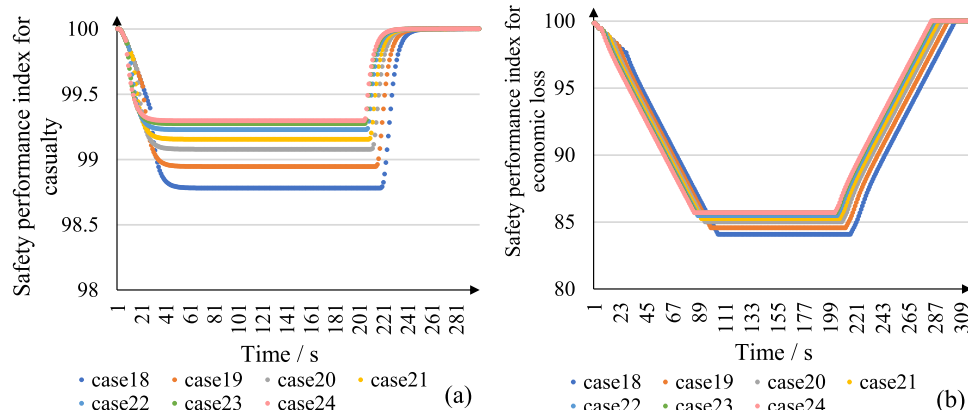


**Fig. 13.** Safety performance curves of different sensor layouts with equal intervals.

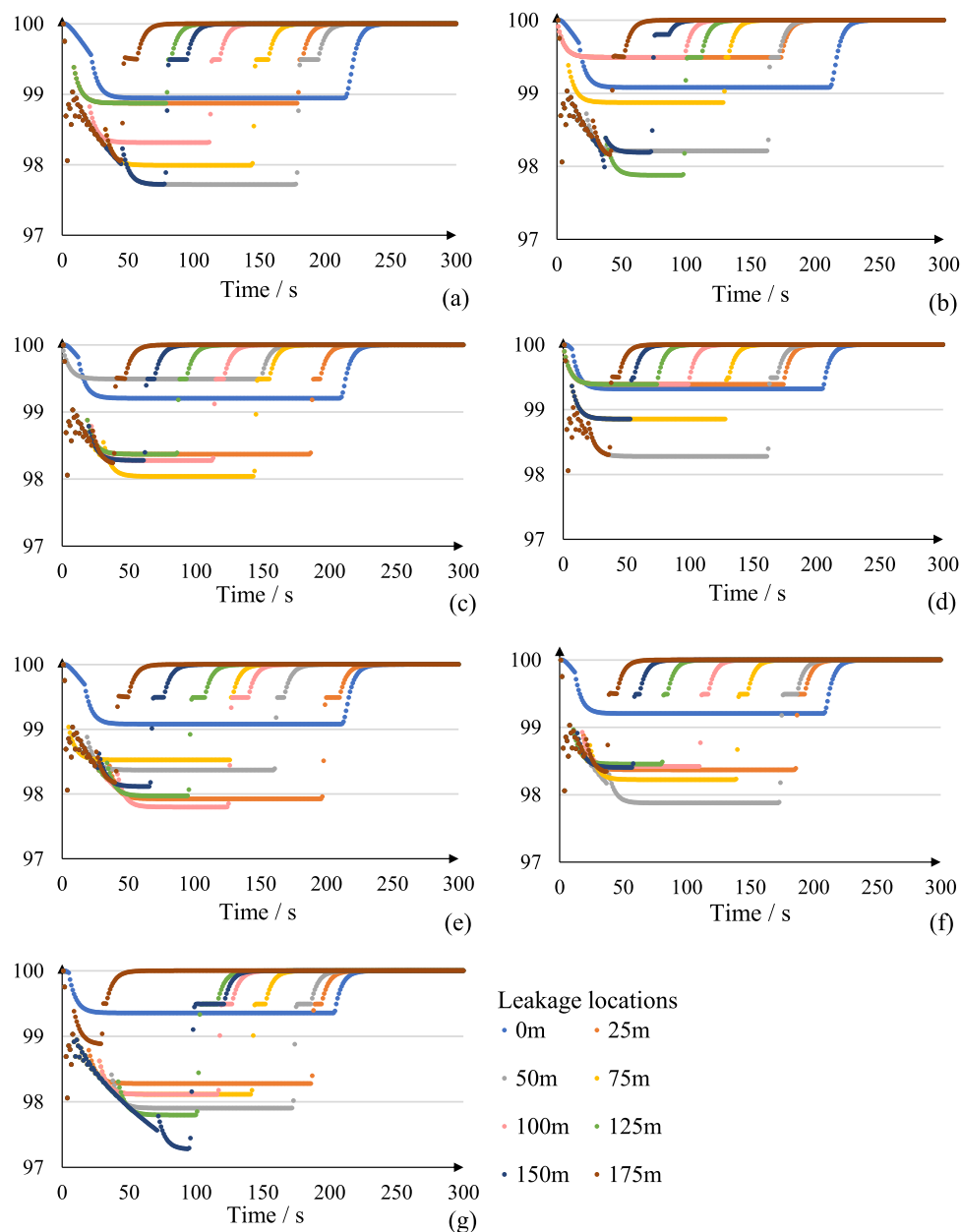


Fig. 14. Safety performance curves for casualty of 7 cases with 8 leakage locations (where (a) is case 19, and (b) to (g) are cases 25–30).

leakage rates, air velocity, sensor layouts, and distance between ESD valves, exhaustive cases are required to identify the optimal emergency strategy. In this work, 9 cases for ventilation strategy and 13 cases for sensor layout are relatively involved in determining the optimal emergency strategy. Meanwhile, the optimal emergency strategy could be identified more accurately by applying more computational resources to the proposed framework with a three-dimensional gas leakage simulation (considering different leakage directions, sizes, and shapes).

The resilience of the natural gas compartment is measured considering casualty and economic loss, respectively. As shown in Fig. 6 and Fig. 8, although resilience metrics of the two aspects are both based on the gas concentration field, they are not consistent since the mechanism of the two kinds of accidents varies. Despite the left part (concentration lower than 20% VOL) of the two metrics being relatively the same, when the concentration reaches 20% VOL, even their trend is different. Such diversity results in the different safety performance curves of two aspects, which means the optimal safety barrier arrangement of the two aspects is not identical in a short time at the very early stage. However,

such diversity only affects the system resilience very slightly. It will be out of work after seconds, which means the optimal emergency strategies proposed in this paper are still applicable.

What the authors proposed in this paper is a dynamic approach for quantifying the system resilience to measure the safety performance considering the whole evolution process, namely degradation, adaptation, and restoration. Such a dynamic and rapid model is difficult to comprehensively take into account all the influencing factors, so, some factors are neglected in this paper, like flame and heat radiation of explosion and three-dimensional gas concentration, which are more detailed analyzed in traditional numerical simulation work and experimental research (Cai et al., 2022; Wu et al., 2020; Zhao et al., 2022).

In the future, Monte Carlo simulation can be applied to conduct a stochastic analysis of leakage location, hole size, staff appearance, and the probability of failure on demand (PFD) of safety barriers to reduce the uncertainty and identify the optimal emergency strategies precisely. Also, adjusting the gas concentration field calculated by numerical simulation through the concentration detected by sensors could be

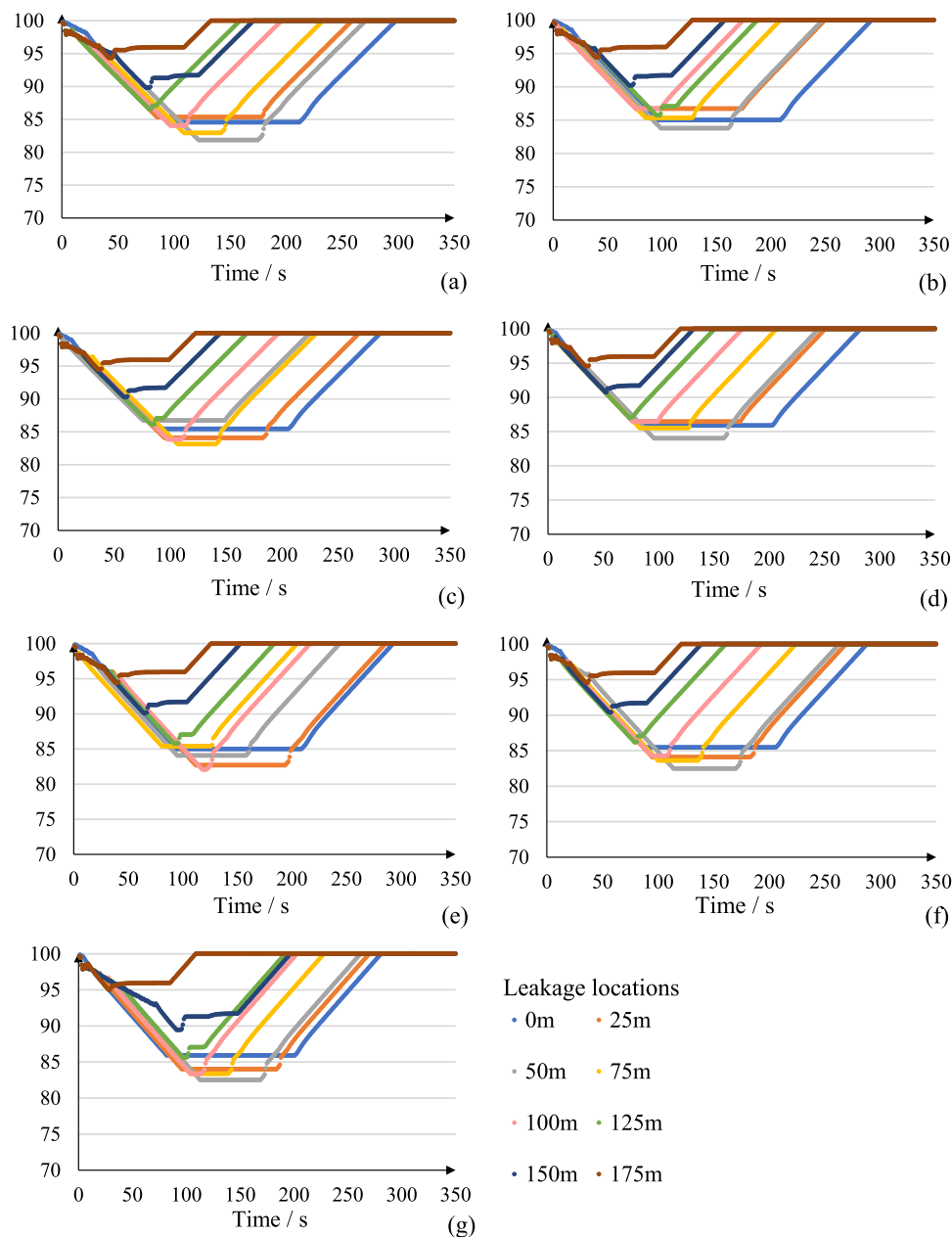


Fig. 15. Safety performance curves for economic loss of 7 cases with 8 leakage locations (where (a) is case 19, and (b) to (g) are cases 25–30).

feasible for real-time resilience modeling. Cost-benefit analysis of safety barriers, comprehensive resilience modeling of the whole utility tunnel, and quantification of coupling accidents in the utility tunnels should also be conducted in the future.

**5. Conclusion**

As a critical infrastructure of cities and industrial parks, the utility tunnel transports natural gas. Natural gas is explosive, flammable, and asphyxiant that might result in serious consequences, but the resilience of utility tunnels has not been assessed yet. In this paper, a novel resilience assessment model of the natural gas compartment of the utility tunnel is proposed. By conducting interacting barrier modeling, gas leakage and dispersion simulation, and safety performance assessment, the resilience with respect to casualties and economic loss is dynamically quantified, and emergency strategies are optimized. The main conclusions of this work are the following:

(1) The proposed model determines the resilience index for the

natural gas compartment based on the spatial-temporal distribution of gas concentration obtained by CFD, considering interacting behaviors of safety barriers, including sensors, ventilation systems, and ESD systems, to realize systematic modeling and resilience-based emergency optimization. The case study indicates that it is an effective approach for dynamic resilience assessment and can also be applied to other confined spaces where hazardous gas may leak, such as road tunnels, metro tunnels, chemical parks, etc.

(2) A delay effect of safety barriers is noticed in this work, showing that the safety performance of the natural gas compartment cannot start to recover simultaneously with barrier activation. For the typical ventilation strategy (0.333 m/s and 0.667 m/s), the delay will be longer than 240 s in the case of upwind leakage. The potential reasons for the delay effect are the gradual decrease of gas release rate after ESD activation and the time-consuming gas dilution process. Enhancing air velocity, increasing sensor density, and shortening the ESD valve interval may reduce the delay effect.

(3) It is found that increasing the air velocity of emergency

ventilation to 1 m/s while maintaining the ordinary air velocity as 0.333 m/s is the optimal ventilation strategy for the natural gas compartment. In this case, the resilience index for casualty increases from 0.863 to 0.992, the resilience for economic loss increases from 0.818 to 0.942, and the delay time of performance recovery drops from 318 s to 170 s. The continuous boost of emergency ventilation can still increase the resilience but only marginal.

(4) Another new finding is that the current specification of sensor density can be reduced from 14 sensors per fire zone (less than 15 m intervals) to 10 sensors (20 m intervals), such change can save 28.57% of sensors with less than 0.51% resilience lost. Moreover, the results indicate that an unequal interval layout of sensors could be more resilient than the current equal ones, the identified optimal sensor layout should be 10 sensors in a 200-m compartment arranged in an arithmetic progression interval:  $8.75 + 2.5(n-1)$ , where  $n$  is the number of sensors from 1 to 10.

### Declaration of Competing Interest

The authors declare that they have no known competing financial interests or personal relationships that could have appeared to influence the work reported in this paper.

### Acknowledgements

This work was supported by Beijing Nova Program (Grant No. Z201100006820072), the National Natural Science Foundation of China (Grant No. 52174223), and the China Scholarship Council (Grant No. 202106430016).

### References

- Ahmadi, S., Saboohi, Y., Vakili, A., 2021. Frameworks, quantitative indicators, characters, and modeling approaches to analysis of energy system resilience: a review. *Renew. Sust. Energ. Rev.* 144, 110988 <https://doi.org/10.1016/j.rser.2021.110988>.
- Amin, M.T., Khan, F., Amyotte, P., 2019. A bibliometric review of process safety and risk analysis. *Process Saf. Environ. Prot.* 126, 366–381. <https://doi.org/10.1016/j.psep.2019.04.015>.
- Azadeh, A., Salehi, V., 2014. Modeling and optimizing efficiency gap between managers and operators in integrated resilient systems: the case of a petrochemical plant. *Process Saf. Environ. Prot.* 92, 766–778. <https://doi.org/10.1016/j.psep.2014.02.004>.
- Azadeh, A., Salehi, V., Ashjari, B., Saberi, M., 2014. Performance evaluation of integrated resilience engineering factors by data development analysis: the case of a petrochemical plant. *Process Saf. Environ. Prot.* 92, 231–241. <https://doi.org/10.1016/j.psep.2013.03.002>.
- Azadeh, A., Yazdanparast, R., Zadeh, S.A., Zadeh, A.E., 2017. Performance optimization of integrated resilience engineering and lean production principles. *Expert Syst. Appl.* 84, 155–170. <https://doi.org/10.1016/j.eswa.2017.05.012>.
- Baalispang, T., Abbassi, R., Garaniya, V., Khan, F., Dadashzadeh, M., 2019. Modelling an integrated impact of fire, explosion and combustion products during transitional events caused by an accidental release of LNG. *Process Saf. Environ. Prot.* 128, 259–272. <https://doi.org/10.1016/j.psep.2019.06.005>.
- Bai, Y.P., Zhou, R., Wu, J.S., 2020. Hazard identification and analysis of urban utility tunnels in China. *Tunn. Undergr. Space Technol.* 106, 103584 <https://doi.org/10.1016/j.tust.2020.103584>.
- Bento, F., Garotti, L., Mercado, M.P., 2021. Organizational resilience in the oil and gas industry: a scoping review. *Saf. Sci.* 133, 105036 <https://doi.org/10.1016/j.ssci.2020.105036>.
- Brittain, D.R., Gyurcsik, N.C., Cary, M.A., Moser, E.N., Davis, L.S., 2021. Differences in resilience mechanisms and physical activity among women experiencing chronic pain with higher or lower resilience. *Women Health Iss.* <https://doi.org/10.1016/j.whi.2021.11.004>.
- Bu, F.X., Liu, Y., Wang, Z.X., Xu, Z., Chen, S.Q., Hao, G.W., Guan, B., 2021. Analysis of natural gas leakage diffusion characteristics and prediction of invasion distance in utility tunnels. *J. Nat. Gas. Sci. Eng.* 96, 104270 <https://doi.org/10.1016/j.jngse.2021.104270>.
- Cai, B., Zhang, Y., Wang, H., Liu, Y., Ji, R., Gao, C., et al., 2021. Resilience evaluation methodology of engineering systems with dynamic-Bayesian-network-based degradation and maintenance. *Reliab. Eng. Syst. Saf.* 209, 107464 <https://doi.org/10.1016/j.ress.2021.107464>.
- Cai, J.T., Wu, J.S., Yuan, S.Q., Liu, Z., Kong, D.S., 2021. Numerical analysis of multi-factors effects on the leakage and gas diffusion of gas drainage pipeline in underground coal mines. *Process Saf. Environ. Prot.* 151, 166–181. <https://doi.org/10.1016/j.psep.2021.05.017>.
- Cai, J.T., Wu, J.S., Yuan, S.Q., Kong, D.S., Zhang, X.L., 2022. Prediction of gas leakage and dispersion in utility tunnels based on CFD-EnKF coupling model: a 3D full-scale application. *Sustain. Cities Soc.* 80, 103789 <https://doi.org/10.1016/j.scs.2022.103789>.
- Cano-Hurtado, J.J., Canto-Perello, J., 1999. Sustainable development of urban underground space for utilities. *Tunn. Undergr. Space Technol.* 14 (3), 335–340. [https://doi.org/10.1016/S0886-7798\(99\)00048-6](https://doi.org/10.1016/S0886-7798(99)00048-6).
- Canto-Perello, J., Curiel-Esparza, J., Calvo, V., 2013. Criticality and threat analysis on utility tunnels for planning security policies of utilities in urban underground space. *Expert Syst. Appl.* 40 (11), 4707–4714. <https://doi.org/10.1016/j.eswa.2013.02.031>.
- Chen, C., Yang, M., Reniers, G., 2021. A dynamic stochastic methodology for quantifying HAZMAT storage resilience. *Reliab. Eng. Syst. Saf.* 215, 107909 <https://doi.org/10.1016/j.ress.2021.107909>.
- Cozzani, V., Salzano, E., 2004. The quantitative assessment of domino effects caused by overpressure: Part I. Probit Models. *J. Hazard. Mater.* A107, 67–80. <https://doi.org/10.1016/j.jhazmat.2003.09.013>.
- Dell'Isola, M., Ficco, G., Lavalle, L., Moretti, L., Tofani, A., Zuena, F., 2020. A resilience assessment simulation tool for distribution gas networks. *J. Nat. Gas. Sci. Eng.* 84, 103680 <https://doi.org/10.1016/j.jngse.2020.103680>.
- Department of Emergency Management of Hubei Province, 2021. Investigation report on the “6-13” major gas explosion accident in Yanhu market, Zhangwan District, Shiyan City, Hubei Province. <http://yj.hubei.gov.cn/yjgl/aqsc/sgdc/202109/P020211002415958135749.pdf> (accessed 27th January 2022 in Chinese).
- Dong, Y., Gao, H., Zhou, J., et al., 2003. Mathematical modeling of gas release through holes in pipelines. *Chem. Eng. J.* 92 (1), 237–241. [https://doi.org/10.1016/S1385-8947\(02\)00259-0](https://doi.org/10.1016/S1385-8947(02)00259-0).
- Duchek, S., 2020. Organizational resilience: a capability-based conceptualization. *Bus. Res.* 13, 215–246. <https://doi.org/10.1007/s40685-019-0085-7>.
- Emenike, S.N., Falcone, G., 2020. A review on energy supply chain resilience through optimization. *Renew. Sust. Energ. Rev.* 134, 110088 <https://doi.org/10.1016/j.rser.2020.110088>.
- Fang, W.P., Wu, J.S., Bai, Y.P., Zhang, L.B., Reniers, G., 2019. Quantitative risk assessment of a natural gas pipeline in an underground utility tunnel. *Process Saf. Prog.* 38, e12051 <https://doi.org/10.1002/prs.12051>.
- FEMA, 2003. Risk management series reference manual to mitigate potential terrorist attacks against buildings. <https://www.fema.gov/pdf/plan/prevent/rms/426/fema426.ch4.pdf>. (Accessed 10th February 2022).
- GB50838, 2015. Technical code for urban utility tunnel engineering. China planning press, Beijing.
- Golara, A., Esmaily, A., 2017. Quantification and enhancement of the resilience of infrastructure networks. *J. Pipeline Syst. Eng. Pract.* 8 (1), 04016013. [https://doi.org/10.1061/\(ASCE\)PS.1949-1204.0000250](https://doi.org/10.1061/(ASCE)PS.1949-1204.0000250).
- Health and Safety Executive, 2010. Methods of Approximation and Determination of Human Vulnerability for Offshore Major Accident Hazard Assessment. [http://www.hse.gov.uk/foi/internalops/hid\\_circs/technical\\_osd/spc\\_tech\\_osd\\_30/spctecod30.pdf](http://www.hse.gov.uk/foi/internalops/hid_circs/technical_osd/spc_tech_osd_30/spctecod30.pdf). (Accessed 26th January 2022).
- Highways, 2015. Thousands evacuated as utility tunnel fire rages. <https://www.highwaysmagazine.co.uk/article/detail/2070>. (accessed 27th January 2022).
- Hu, J., Khan, F., Zhang, L., 2021. Dynamic resilience assessment of the Marine LNG offloading system. *Reliab. Eng. Syst. Saf.* 208, 107368 <https://doi.org/10.1016/j.ress.2020.107368>.
- Liaw, H.J., 2016. Lessons in process safety management learned in the Kaohsiung gas explosion accident in Taiwan. *Process Saf. Prog.* 35 (3), 228–232. <https://doi.org/10.1002/prs.11818>.
- Liu, H., Mao, S., Li, M., 2019. A Case Study of an Optimized Intermittent Ventilation Strategy Based on CFD Modeling and the Concept of FCT. *Energies* 12 (4), 721. <https://doi.org/10.3390/en12040721>.
- Liu, W., Song, Z., 2020. Review of studies on the resilience of urban critical infrastructure networks. *Reliab. Eng. Syst. Saf.* 193, 106617 <https://doi.org/10.1016/j.ress.2019.106617>.
- MOHURD (Ministry of Housing and Urban-Rural Development of the People's Republic of China), 2011. Technical Specification for Gas Alarm and Control System in China (CJJ/T 146–2011). [https://www.mohurd.gov.cn/gongkai/fdzdgknr/tzgg/201112/20111221\\_208046.html](https://www.mohurd.gov.cn/gongkai/fdzdgknr/tzgg/201112/20111221_208046.html). (Accessed 15th February 2022 in Chinese).
- MOHURD (Ministry of Housing and Urban-Rural Development of the People's Republic of China), 2015. Construction investment estimation index of urban utility tunnels (ZYA1–12(10)–2015). [https://www.mohurd.gov.cn/gongkai/fdzdgknr/tzgg/201506/20150629\\_222705.html](https://www.mohurd.gov.cn/gongkai/fdzdgknr/tzgg/201506/20150629_222705.html). (Accessed 11th February 2022 in Chinese).
- Pawar, B., Park, S., Hu, P., Wang, Q., 2021. Applications of resilience engineering principles in different fields with a focus on industrial systems: a literature review. *J. Loss Prev. Process Ind.* 69, 104366 <https://doi.org/10.1016/j.jlp.2020.104366>.
- Pekalski, A.A., Schildberg, H.P., Smallegange, P.S.D., Lemkowitz, S.M., Zevenbergen, J. F., Braithwaite, M., Pasman, H.J., 2005. Determination of the explosion behaviour of methane and propane in air or oxygen at standard and elevated conditions. *Process Saf. Environ. Prot.* 83 (B5), 421–429. <https://doi.org/10.1205/psep.04211>.
- Penalozka, G.A., Formoso, C.T., Saurin, T.A., 2021. A resilience engineering-based framework for assessing safety performance measurement systems: a study in the construction industry. *Saf. Sci.* 142, 105364 <https://doi.org/10.1016/j.ssci.2021.105364>.
- Psyras, N., Sextos, A., 2018. Safety of buried steel natural gas pipelines under earthquake-induced ground shaking: a review. *Soil Dyn. Earthq. Eng.* 106, 254–277. <https://doi.org/10.1016/j.soildyn.2017.12.020>.
- Saikia, P., Beane, G., Garriga, R.G., Avello, P., Ellis, L., Fisher, S., 2022. City water resilience framework: a governance based planning tool to enhance urban water

- resilience. *Sustain. Cities Soc.* 77, 103497 <https://doi.org/10.1016/j.scs.2021.103497>.
- Salehi, V., Veitch, B., 2020. Performance optimization of integrated job-driven and resilience factors by means of a quantitative approach. *Int. J. Ind. Ergon.* 78, 102987 <https://doi.org/10.1016/j.ergon.2020.102987>.
- Sang, M., Ding, Y., Bao, M., Li, S., Ye, C., Fang, Y., 2021. Resilience-based restoration strategy optimization for interdependent gas and power networks. *Appl. Energ.* 302, 117560 <https://doi.org/10.1016/j.apenergy.2021.117560>.
- Sarwar, A., Khan, F., James, L., Abimbola, M., 2018. Integrated offshore power operation resilience assessment using Object Oriented Bayesian network. *Ocean Eng.* 167, 257–266. <https://doi.org/10.1016/j.oceaneng.2018.08.052>.
- Sciencing, 2018. Minimum Oxygen Concentration for Human Breathing. <https://sciencing.com/minimum-oxygen-concentration-human-breathing-15546.html>. (Accessed 10th February 2022).
- Serdar, M.Z., Koç, M., Al-Ghamdi, S.G., 2022. Urban transportation networks resilience: indicators, disturbances, and assessment methods. *Sustain. Cities Soc.* 76, 103452 <https://doi.org/10.1016/j.scs.2021.103452>.
- Sesini, M., Giarola, S., Hawkes, A.D., 2020. The impact of liquefied natural gas and storage on the EU natural gas infrastructure resilience. *Energy* 209, 118367. <https://doi.org/10.1016/j.energy.2020.118367>.
- Su, H., Zhang, J., Zio, E., Yang, N., Li, X., Zhang, Z., 2018. An integrated systemic method for supply reliability assessment of natural gas pipeline networks. *Appl. Energ.* 209, 489–501. <https://doi.org/10.1016/j.apenergy.2017.10.108>.
- Vairo, T., Pontiggia, M., Fabiano, B., 2021. Critical aspects of natural gas pipelines risk assessments. A case-study application on buried layout. *Process Saf. Environ. Prot.* 149, 258–268. <https://doi.org/10.1016/j.psep.2020.10.050>.
- Wang, T., Zhou, Y., Luo, Z., Wen, H., Zhao, J., Su, B., 2020. Flammability limit behavior of methane with the addition of gaseous fuel at various relative humidities. *Process Saf. Environ. Prot.* 140, 178–189. <https://doi.org/10.1016/j.psep.2020.05.005>.
- Wang, T.Y., Tan, L.X., Xie, S.Y., Ma, B.S., 2018. Development and applications of common utility tunnels in China. *Tunn. Undergr. Space Tech.* 76, 92–106. <https://doi.org/10.1016/j.tust.2018.03.006>.
- Wu, J.S., Zhou, R., Xu, S.D., Wu, Z.W., 2017. Probabilistic analysis of natural gas pipeline network accident based on Bayesian network. *J. Loss Prev. Process Ind.* 46, 126–136. <https://doi.org/10.1016/j.jlpp.2017.01.025>.
- Wu, J.S., Liu, Z., Yuan, S.Q., Cai, J.T., Hu, X.F., 2020. Source term estimation of natural gas leakage in utility tunnel by combining CFD and Bayesian inference method. *J. Loss Prev. Process Ind.* 68, 104328 <https://doi.org/10.1016/j.jlpp.2020.104328>.
- Wu, J.S., Bai, Y.P., Fang, W.P., Zhou, R., Reniers, G., Khakzad, N., 2021. An integrated quantitative risk assessment method for underground utility tunnels. *Reliab. Eng. Syst. Saf.* 213, 107792 <https://doi.org/10.1016/j.res.2021.107792>.
- Xu, Y., Huang, Y., Li, J., Ma, G., 2021. A risk-based optimal pressure relief opening design for gas explosions in underground utility tunnels. *Tunn. Undergr. Space Technol.* 116, 104091 <https://doi.org/10.1016/j.tust.2021.104091>.
- Yan, Q., Zhang, Y., Sun, Q., 2020. Characteristic study on gas blast loadings in an urban utility tunnel. *J. Perform. Constr. Facil.* 34 (4), 04020076. [https://doi.org/10.1061/\(ASCE\)CF.1943-5509.0001477](https://doi.org/10.1061/(ASCE)CF.1943-5509.0001477).
- Yang, D., Chen, G., Shi, J., Zhu, Y., Dai, Z., 2020. A novel approach for hazardous area identification of toxic gas leakage accidents on offshore facilities. *Ocean Eng.* 217, 107926 <https://doi.org/10.1016/j.oceaneng.2020.107926>.
- Yang, Y., Wu, C., Liu, X., Du, J., Zhang, H., Xu, S., et al., 2021. Protective effect of unbonded prestressed ultra-high performance reinforced concrete slab against gas explosion in buried utility tunnel. *Process Saf. Environ. Prot.* 149, 370–384. <https://doi.org/10.1016/j.psep.2020.11.002>.
- Yao, Y., Fu, B., Liu, Y., Li, Y., Wang, S., Zhan, T., 2022. Evaluation of ecosystem resilience to drought based on drought intensity and recovery time. *Agr. For. Meteorol.* 314, 1088–1089. <https://doi.org/10.1016/j.agrformet.2022.108809>.
- Ye, K., Tang, X., Zheng, Y., Ju, X., Peng, Y., Liu, H., 2021. Estimating the two-dimensional thermal environment generated by strong fire plumes in an urban utility tunnel. *Process Saf. Environ. Prot.* 148, 737–750. <https://doi.org/10.1016/j.psep.2021.01.030>.
- Yuan, S.Q., Wu, J.S., Zhang, X.L., Liu, W.Y., 2019. EnKF-based estimation of natural gas release and dispersion in an underground tunnel. *J. Loss Prev. Process Ind.* 62, 103931 <https://doi.org/10.1016/j.jlpp.2019.103931>.
- Zhang, S., Ma, H., Huang, X., Peng, S., 2020. Numerical simulation on methane-hydrogen explosion in gas compartment in utility tunnel. *Process Saf. Environ. Prot.* 140, 100–110. <https://doi.org/10.1016/j.psep.2020.04.025>.
- Zhang, Y., Cai, B., Liu, Y., Jiang, Q., Li, W., Feng, Q., et al., 2021. Resilience assessment approach of mechanical structure combining finite element models and dynamic Bayesian networks. *Reliab. Eng. Syst. Saf.* 216, 108043 <https://doi.org/10.1016/j.res.2021.108043>.
- Zhao, Y.M., Wu, J.S., Zhou, R., Cai, J.T., Bai, Y.P., Pang, L., 2022. Effects of the length and pressure relief conditions on propagation characteristics of natural gas explosion in utility tunnels. *J. Loss Prev. Process Ind.* 75, 104679 <https://doi.org/10.1016/j.jlpp.2021.104679>.
- Zhu, W., Li, B., Han, Z., 2021. Synergistic analysis of the resilience and efficiency of China's marine economy and the role of resilience policy. *Mar. Policy* 132, 104703. <https://doi.org/10.1016/j.marpol.2021.104703>.
- Zhu, Y., Wang, D., Shao, Z., Zhu, X., Xu, C., Zhang, Y., 2020. Investigation on the overpressure of methane-air mixture gas explosions in straight large-scale tunnels. *Process Saf. Environ. Prot.* 135, 101–112. <https://doi.org/10.1016/j.psep.2019.12.022>.